Ultrastructural Analysis of Buckwheat Starch Components Using Atomic Force Microscopy

Suresh Neethirajan, Kazumi Tsukamoto, Hiroko Kanahara, and Shigeru Sugiyama

Abstract: Morphological and structural features of buckwheat starch granules and nanocrystals were examined using atomic force microscopy and dynamic light scattering. Partially digested starch granules revealed a clear pattern of growth rings with the central core revealing lamellar structure. Atomic force microscopy and dynamic light scattering experiments revealed that the buckwheat starch granules were polygonal in shape and were in the range of 2 to 19 μm in diameter. The optimized acid hydrolysis process produced nanocrystals with the shape of spherical structure with lengths ranging from 120 to 200 nm, and the diameter from 4 to 30 nm from aqueous suspensions of buckwheat starch solution. The sorption isotherms on buckwheat starch nanocrystal/glycerol composite exhibited a 3-stage transition of moisture in the blending. The biocompatible nature of buckwheat starch nanocrystals and their structural properties make them a promising green nanocomposite material.

Keywords: atomic force microscopy, bionanocomposites, buckwheat, starch granules, starch nanocrystals

Practical Application: Buckwheat starches had never been studied on a nanoscale, but we have achieved new understanding of starch granule morphology and concentric growth rings using nanoscale imaging. Since buckwheat is an underutilized crop, we foresee the potential application of buckwheat starch, starch-based nanocrystals, and nanoparticles, to expand markets and encourage producers to expand their buckwheat acreage. The atomic force image analysis suggests that buckwheat starch could be used as a new biopolymer material in food industries.

Introduction

Bio-based nanoparticles and nanocomposites are gaining momentum in the food packaging industry because of their natural, renewable, and biodegradable properties. Starch is the major source of carbohydrate and the most abundant polysaccharide in plants. The micro- and nanoscale structure of starch granules influences the biological and the physicochemical properties of food (Fredriksson and others 1998; Aguilera and Stanley 1999; Lindeboom and others 2004). Particle size of starch granules contributes to specific functional qualities such as texture, volume, consistency, and moisture and shelf stability (Raeker and others 1998). In addition, the size of starch granules affects the temperatures of gelatinization, which in turn influences the properties of food (Soral-Smietana and others 1984). Enhanced understanding of the structure and morphology of starch granules aids in the selection of processing parameters in the food industry, and opens up new avenues of biomedical applications.

Being a biodegradable, nontoxic, abundant, and cheaper material, starch is preferred over synthetic polymers. New nontraditional applications and technologies based on starch are emerging. Nanoparticles and nanocrystals synthesized from starch exhibit reinforced thermal, higher temperature resistance, and mechanical and barrier properties (Le Corre and others 2010; Szymonska and others 2009). Because of these unique characteristics, starch nanocrystals and nanoparticles are becoming important for potential applications in food science and medicine sector. Starch-based nanoparticles and nanocrystals are also used as biodegradable packing filler (Franciscus and others 2004); as a vector for transport of molecules with biological activity; as an encapsulation material in the food and drug delivery system (Shimoni 2008); and as a food packaging material (Le Corre and others 2010). Nanocomposites are new classes of materials that incorporate either nanoparticles or nanocrystals to increase the higher surface to volume ratio of the reinforcing phase of the matrix. In addition, the nanometric fillers such as the nanocrystals or nanoparticles dispersed into the matrix improve the mechanical stiffness, and the gas barrier properties of the composites.

Buckwheat (*F. esculentum* or Common Buckwheat) is an underutilized crop and has been grown in several hundreds of hectares in Asia, Eastern and Central Europe, and in North America. Because of the nutritious advantages of buckwheat, this crop has been considered as a raw material for functional food and medicine. Buckwheat is consumed in the form of flour for making noodles, pancakes, and pasta; and, as whole-seed groats for making porridge, salad, and tea. Minor crops are usually less investigated and hence the information on the ultrastructural details of buckwheat starch is limited. The size and shape of starch granules are species-specific (Stark and Lynn 1992). Investigation of physical properties of buckwheat starch components is essential for the assessment of development of new food and nontraditional biopolymer-based products.

MS 20110829 Submitted 7/10/2011, Accepted 9/5/2011. *Author Neethirajan is with Biological and Nanoscale Systems Group, Biosciences Div., Oak Ridge National Laboratory, Oak Ridge, TN 37831-6445, U.S.A. Authors Tsukamoto, Kanahara and Sugiyama are with the Nanobiotechnology Laboratory, National Food Research Inst., 2-1-12 Kannondai, Tsukuba, Ibaraki 305-8642, Japan. Direct inquiries to author Neethirajan (E-mail: s.neethi@uoguelph.ca).*

doi: 10.1111/j.1750-3841.2011.02442.x

Journal of Food Science A Publication of the Institute of Food Technologists

Atomic Force Microscopy (AFM) has been proved to be a powerful tool to study biomacromolecules (Baldwin and others 1998; Szymonska and others 2000; Neethirajan and others 2008). Our study sets out to explore the synthesis of nanocrystals and nanoparticles from buckwheat starch, with the main focus concerning the characterization of the buckwheat starch on the nanoscale. More specifically, the aim of our study was to accurately investigate the buckwheat starch granule surface nanostructure using AFM, and characterize the morphological features of buckwheat starch granules, starch-based nanocrystals, and nanoparticles. Furthermore, the influence of the nanocrystal in the glycerol-starch nanocrystal composites was investigated by the moisture-uptake isotherms.

Materials and Methods

Isolation of starch

Buckwheat starch was isolated from flour by steeping 300 g flour in 0.2% NaOH (1:6; w/v) in a 45 °C water bath for 90 min. The flour was then blended for 2 min and screened and centrifuged at 3000 × *g* for 15 min. The supernatant was discarded and the top yellow protein layer was removed. The white starch layer was resuspended in distilled water and centrifuged, and the protein layer was removed. This process was repeated until the yellow layer was no longer visible. The sedimented starch was resuspended in distilled water, adjusted to pH 6.5 to7.0 with dilute HCl, and centrifuged. The starch was washed with distilled water 3 times and air-dried.

Preparation of starch nanocrystals

Acid hydrolysis process (Angellier-Coussy and others 2009) was employed for modifying the starch and preparing the nanocrystals. Briefly, buckwheat starch (37 g) was mixed with 250 mL of 3.16 M H_2SO_4 and continuously stirred at 100 rpm in a shaker for 5 days at 40 °C. The suspension was then cooled down to room temperature, washed by successive centrifugations in distilled water until neutral, followed by mechanical treatment, and freeze-dried using liquid nitrogen.

Preparation of starch nanoparticles

Buckwheat starch (8 g) was added into 150 mL of distilled water. The mixture was heated at 90 °C for 90 min in a shaking water bath at 100 rpm. Ethanol (150 mL) was added dropwise with constant stirring and the solution was allowed to cool down. Upon reaching the room temperature, additional 150 mL of ethanol was added dropwise for 45 min. The suspensions were centrifuged at 8000 rpm for 30 min, and the settled nanoparticles were washed again to remove the water. The samples were kept in a covered petri dish and allowed to dry at 50 °C for removing the ethanol. The acid and the alcohol concentration, temperature, and time were optimized during the synthesis process for the size and yield of both the starch nanocrystals and nanoparticles.

Dynamic light scattering (DLS) measurements

Particle size distribution of starch granules was characterized using a particle sizer (SALD-7100, Shimadzu Corp., Kyoto, Japan) with an ultraviolet laser (wavelength $\lambda = 375$ nm) as a light source. The starch suspension solution (10 mg/mL) was prepared by placing dry starch granules in distilled water with stirring at 150 rpm. The supernatant containing the dispersed starch granules was separated from the sediments and used for the light scattering experiments. All measurements were performed at 25 °C.

Sample preparation for AFM imaging. Starch granules were embedded in LR white resin (London Resin, Basingstoke, U.K.) at 45°C in polyurethane capsules. Two micrometer thin sections were cut with a stainless steel microtome knife using Leica Ultramicrotome (Leica RM2265, Wetzlar, Germany). Then, the thin-sectioned samples were attached to a clean glass slide and were ready for imaging. The nanocrystal sample solution was prepared by dissolving freeze-dried starch crystals (10 mg) in 2 mL of water. The dispersions were then obtained through ultrasonic treatment of the crystal solution for 10 s followed by filtration through 0.45-μm micropore filter. The filtered solution was deposited on a freshly cleaved mica sheet, washed with deionized water gently, and air-dried before imaging. Similarly, the nanoparticle solutions were filtered using 0.45-μm millipore filter and then deposited on a freshly cleaved mica substrate and were air-dried before imaging.

Preparation of nanocomposite films

Nanocomposite films were prepared according to Cao and others (2008). Briefly, a mixture of dry buckwheat starch powder and glycerol (36 wt%) was heated to 100 °C for 30 min, followed by cooling to 70 °C, and then casted in a petri dish followed by drying in an oven at 50 °C. The nanocrystals were added during casting over a range of 10, 20, 30, and 40 wt% to obtain various compositions of nanocomposite films. As a control, buckwheat starch without adding the nanocrystals was prepared using the above procedure. Small strips (50 mm × 10 mm × 0.5 mm) of the above castings were used for the water absorption kinetics study.

Water absorption isotherms and kinetics

Moisture sorption isotherms were determined as described by Kristo and Biliaderis (2007). Small strips of about 300 mg of nanocomposite films were placed in aluminum dishes, dried at 45 °C in an oven. Different saturated salt solutions ($KC_2H_3O_2$, $LiNO_3$, NaBr, KCl, K_2SO_4) were prepared in the individual sealed containers to create the specific relative humidity (Rockland 1960) at 25°C. The moisture content of samples after storage was determined by drying at 110 °C for 2 hours and the data were fitted to the Guggenheim-Anderson-deBoer (GAB) sorption isotherm model.

Imaging

To get a prior knowledge of the sampling area at high resolution for AFM imaging and to ensure sample representativity, the buckwheat starch granules were imaged using a Phase Contrast Microscope (Model BX50, Olympus Corp., Tokyo, Japan) and a Scanning Electron Microscope (SEM). The starch samples were coated with a thin layer of gold to provide conductivity of the specimen, and the imaging was performed by a JSM-6000F (JEOL, Tokyo, Japan) SEM. AFM (Nanowizard, JPK Instruments, Berlin, Germany) was used for obtaining nanoscale images of starch granules and the nanocrystals. Standard silicon cantilevers (Olympus Corporation, Tokyo, Japan) with a spring constant of $k = 42$ Nm^{-1} were used. All AFM measurements were carried out in atmospheric air at room temperature (25 °C) using the intermittent contact mode with resonant frequency around 300 kHz. The scan speeds were in the range of 0.2 to 0.3 Hz. Both topographic and error signal images were acquired simultaneously during AFM imaging. The analysis and measurement of the images were made using SPIP software (Image Metrology, Copenhagen, Denmark).

Results and Discussion

SEM and DLS analysis (Figure 1a, 1b) of the buckwheat starch granules suggest that the granules are polygonal in shape and their

size is in the range of 2 to 19 μm. The size and shape comparison of buckwheat starch with wheat, corn, and pea starch granules (Table 1) shows that buckwheat starch are characteristically different and about 2.4 times smaller than the wheat and corn starch granules. Buckwheat starch is also different in terms of the amylopectin-amorphous ratio as well as the size, shape, and its functional attributes in relation to the wheat, barley, and corn starches. Unlike corn and wheat starch, buckwheat is composed of a glucoside named rutin (Couch and others 1946).

The rough seed coat and the crumbling nature of seed during sectioning did not permit to image the internal structure of starch directly within buckwheat seeds. It is recognized that the embedding using resin may penetrate into the starch granules leading to cross-linked structures (Ridout and others 2002). This resin penetration was carefully avoided by selecting proper region of interest for imaging through phase-contrast microscope and by multiple sampling. AFM image (Figure 2) of starch granules shows the compact arrangement of starch along with few protein bodies. Similar to maize starch, the hilum of buckwheat starch is distinctly visible in the center of the granule. Hilum, the boundary of starch granules, growth rings, and channel-like cavities is clearly visible in the error-signal mode images (Figure 3) than in the topographic AFM images (not shown).

The growth ring structure of the starch granules is visible only in the error-signal mode image (Figure 3), but not in the topography image. The height variation across the growth rings in the topography image is approximately 14 nm. There is an absence of growth rings near the hilum region of the granule. The area

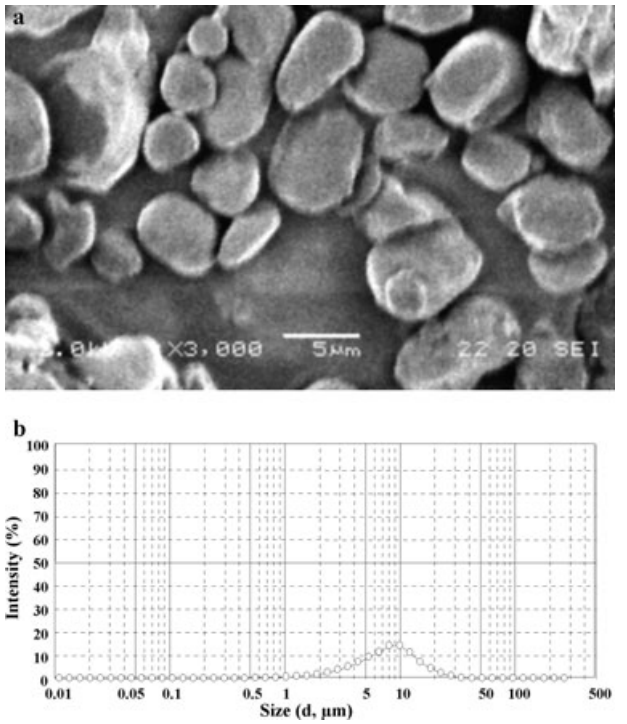

Figure 1–Exterior morphology and particle size distribution of buckwheat starch granules. (a) SEM images of starch granules (3000X); (b) particle size distribution of starch granules in 1.00% (w/w) solution in water at 25°C.

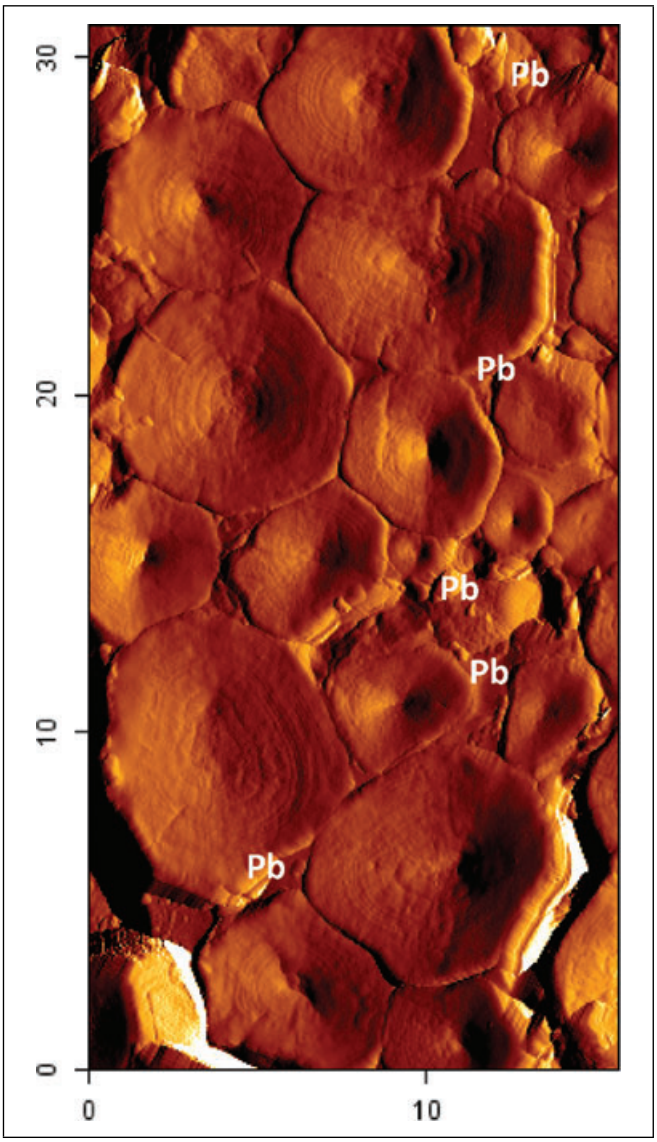

Figure 2–Atomic force microscopy image of buckwheat starch granules (Error-signal mode). Protein bodies (Pb) are recognized from the labeled region.

Table 1–Granule sizes of starches from various botanical origins.

Starch	Average granular size/diameter (μm)	Shape	Crystalline type
Barley (Tang and others 2001)	2 to 3 and 12 to 32	Oval to round	Bimodal (A and B type)
Buckwheat	2 to 17	Polygonal	A
Wheat (Neethirajan and others 2008)	<10 and 10 to 35	Polyhedral	Bimodal (A and B type)
Corn (Baker and others 2001)	2 to 30	Round	A
Rice (Lindeboom and others 2004)	50 to 80	Round	B
Potato (Szymonska and others 2009)	5 to 100	Oval	B
Cassava (Juszczak and others 2003)	3 to 30	Kettle-drum/truncated	A

surrounding the hilum region is more compressed than the rest of the starch granule surface. The outer regions of the starch granules might have expanded more than the central regions due to sectioning. This might result in the variability of compressibility of the hilum between the individual starch granules.

The carbohydrate-starch polymer is made of glucose units consisting of linear amylose and branched amylopectin, and is organized in alternating crystalline and amorphous lamellae in the granules (Myers and others 2000). It has been shown that growth rings are heterogeneous and may possibly arise due to variations in crystallinity of the component polymers (Ridout and others 2004; Parker and others 2008). The growth ring structure of the buckwheat starch granules showing the branched amylopectin molecules is clear and visible in the error-signal mode image (Figure 3a and 3b) but not in the topography image (Figure 3c). Gelatinization and retrogradation properties correlate with unit-chain length distribution of amylopectin (Noda and others 1998; Srichuwong and others 2005). The quantitative molar distributions of amylopectin chain length of buckwheat starch samples analyzed by anion-exchange chromatography (Noda and others 1998) revealed that an increase in short outer chains in amylopectin molecules resulted in lower onset and peak temperature as well as enthalpy change during gelatinization. AFM image analysis of the buckwheat starch granules conforms to the cluster model (Figure 3d) previously proposed for cereal starch granule structures by physicochemical and biological methods (Calvert 1997). Unlike corn or sorghum starch granule surface (Huber and BeMiller 1997), the surface of starch granules was smooth without any cavities or channels due to swelling conditions.

Starch nanocrystals

The structure and the morphology of starch nanocrystals are determined by the botanical origin of the starch and the amylose-amylopectin distribution within the granule (Gerard and others 2002). The remnants and envelopes surrounding the external layers of starch granules during gelatinization process are shown to be varying in amylose/amylopectin ratios and exhibit elastic/plastic properties (Atkin and others 1998). In our study, disruption of amorphous domains from semicrystalline granules using acid hydrolysis process produced starch nanocrystals. The nanocrystals synthesized by varying temperatures between 35 to 45 °C, do not show any change in the morphology or the dimensions. Hence, temperature does not influence the size or the yield of the nanocrystals. The resulting buckwheat starch nanocrystals were spherical in shape, ranging in diameter from 120 to 200 nm, and thicknesses from 4 to 30 nm, respectively. Aggregated as well as isolated, individual spherical nanocrystal AFM images are observed in Figure 4. The aqueous solution of starch nanocrystals exhibited stability and dispersion without flocculation (Figure 5a and 5b). This may be by the sulphate groups on the surface of starch nanocrystals caused due to the acid hydrolysis process.

Nanocomposite films prepared using glycerol as the amorphous matrix and buckwheat starch nanocrystals as the reinforcing phase, were studied for the effect of water activity. The water absorption isotherms and the water barrier properties of buckwheat starch nanocomposite films filled with 0% to 40% (w/w) nanocrystals (nanocrystals + glycerol) are shown in Figure 6.

All the moisture sorption isotherm curves typically display a sigmoidal shape. The sorption isotherms have 3 phases of sorption behavior, the monomolecular layer phase upto 0.3 a_w, multimolecular layer phase from 0.3 to 0.6 a_w, and capillary condensation phase from 0.6 to 1 a_w. With the increase in the starch content and the increase in a_w, the slope of the isotherms increased, due to the higher sorption of water molecules by starch and/or more sorption capacity of starch. In monomolecular phase, the control sample and all combinations of starch nanocrystal-glycerol samples had a tendency to lose moisture upto 0.3 a_w. The moisture uptake appears to be slow as the isosorption values of starch nanocrystals-glycerol films is between the ranges of 0.3 to 0.6 a_w. In the capillary condensation phase, the moisture uptake of the films is quicker. The isotherm curve was found to increase with an increase in the starch content of the nanocrystal-glycerol film,

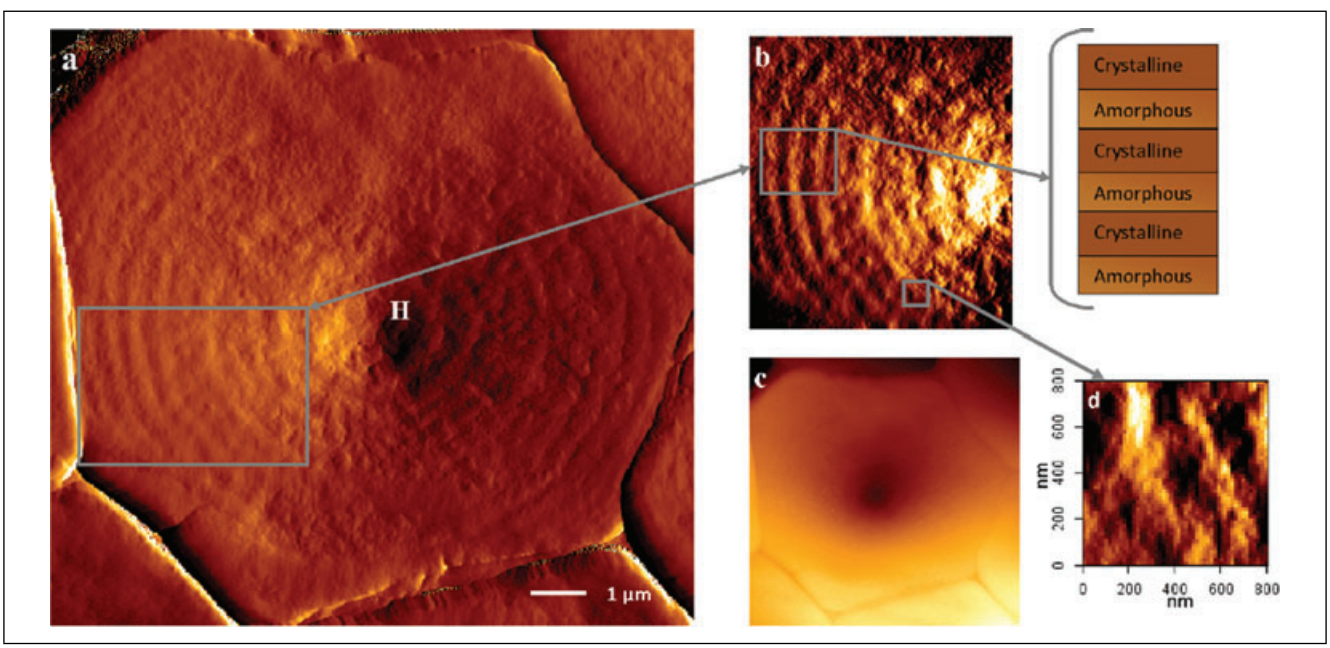

Figure 3–AFM images of buckwheat starch granule. (a) Error-signal mode image and the corresponding topography image (c). 3(b) Growth rings consisting of alternate layers of amorphous and crystalline regions. 3(d) Growth rings exhibit further substructure known as blocklets. H - hilum.

due to the higher moisture absorption capacity of the buckwheat starch. As the concentration of nanocrystals increased, composite films absorbed less water, under similar a_w conditioning, and this difference was more pronounced at high moisture conditions ($a_w > 0.75$). The monolayer moisture decreased and then increased with increasing starch nanocrystals concentration in the film indicating that the nanocrystals behave as hydrophilic centers at which the 1st layer of water molecules is bonded with high binding intensity than the water molecule of the indirectly bonded layer. Researchers have observed similar trend for moisture uptake for low-density polyethylene/starch film and Gliadins polymerized with cysteine (Raj and others 2002; Hernandez-Munoz and others 2004). Because of high surface undulation of the nanocomposite films on the mica substrate, AFM images did not provide useful morphological information about the nanocomposite films.

Starch nanoparticles

Gelatinization process breaks down the intermolecular bonds of starch molecules, causing a change in the crystallinity to yield the starch nanoparticles. Because of the difference in synthesis process, it is expected that the nanoparticles will be of amorphous in nature compared to the crystallinity nature of the buckwheat starch nanocrystals. As observed by AFM (Figure 7), buckwheat starch nanoparticles were spherical in shape. Previous studies have established that the hydrogen ions during the acid hydrolysis process alter the crystalline nature of the granules, and thereby changes the degree of crystallanity (Corre and others 2010). Gelatinization process breaks down the intermolecular bonds of starch molecules, causing a change in the crystallinity to yield the amorphous starch nanoparticles. Penetration of water into the molecules and the higher temperature reduces the crystallanity leading to amorphous nature of starch nanoparticles. Additional studies such as X-ray scattering profiles are necessary to confirm the crystalline and amorphous nature of the nanocrystals and the nanoparticles from buckwheat starch.

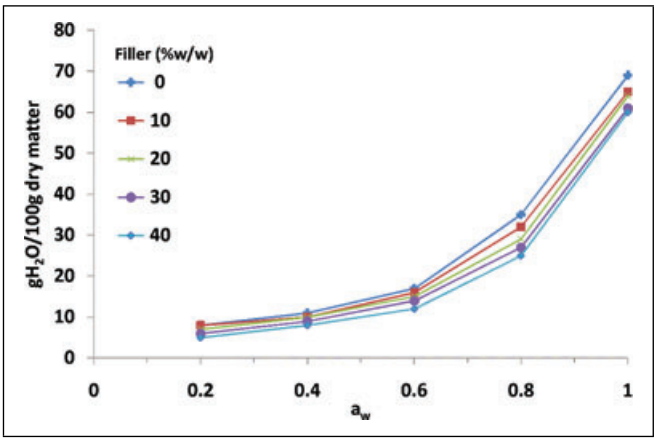

Figure 6–Moisture sorption isotherms of buckwheat starch-glycerol composite films filled with various nanocrystal concentrations. Solid lines represent the GAB model fit to the data.

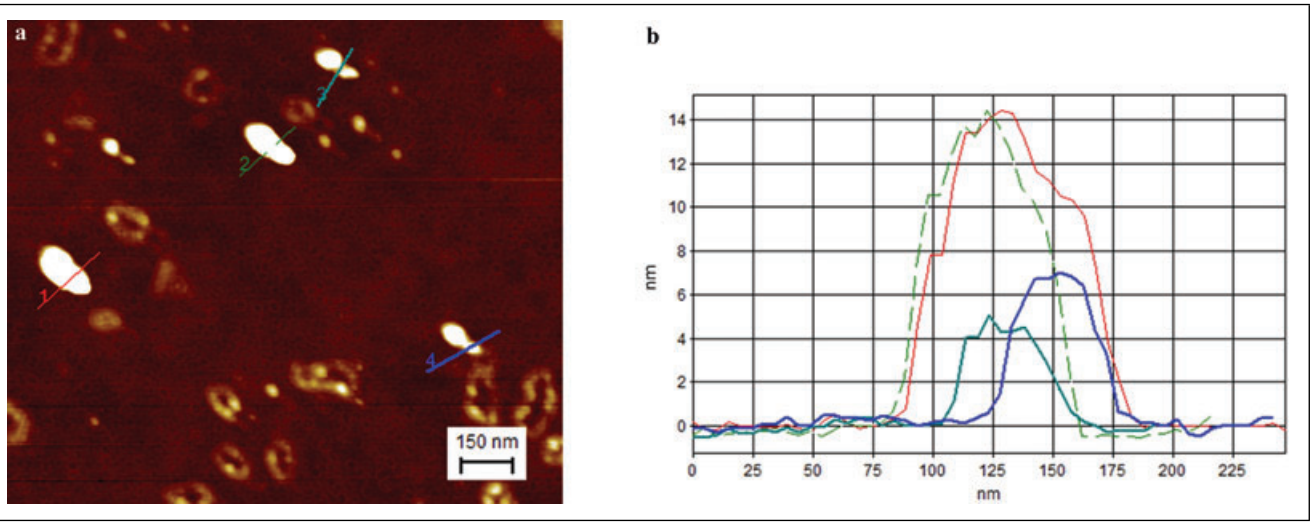

Figure 4–(a) AFM topography image of buckwheat starch nanocrystals after drying on a mica surface, (b) size distribution graph.

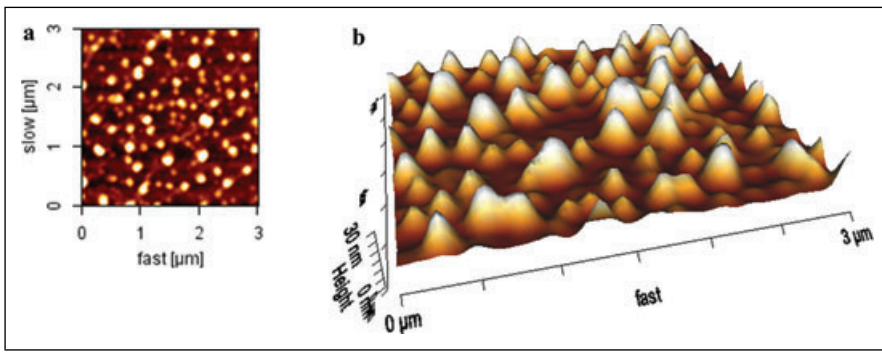

Figure 5–AFM images of the distribution (a) and height profile (b) of nanocrystals on mica substrate.

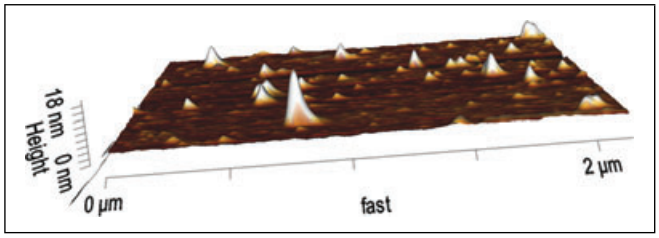

Figure 7–3D AFM height image of buckwheat starch nanoparticles. Raw atomic force microscope data is visualized as 3D surface.

To make use of buckwheat starch nanoparticles and nanocrystals as a new material for industrial applications, further studies are required to understand the reinforcing phenomenon as well as the affinity between the matrix and filler. Nonetheless, due to their biodegradability, and abundance, buckwheat-starch bionanocomposites are promising.

Conclusion

Characterization using AFM and SEM reveals that the buckwheat starch granules are round or polygonal in shape. DLS analysis and AFM image analysis show that the starch granules are in the range of 2 to 19 μm in size. AFM analysis revealed that the buckwheat starch nanocrystals are spherical in shape with thicknesses between 8 and 30 nm and conform to the theory of crystalline lamellae. The sorption isotherms help to understand the influence of nanocrystals on buckwheat-starch nanocrystal/glycerol nanocomposites. In addition, the isotherms facilitate the determination of the tailor-made blends for making water vapor barrier packaging and biopackaging materials. Further tests are required to evaluate the functional properties of buckwheat starch nanocrystals and nanoparticles, such as water vapor permeability, mechanical thermal analysis, and tensile strength and modulus, optical and chemical property to gain confidence for applications in green nanocomposite synthesis. The results of our study open up new opportunities for the underutilized buckwheat as a novel biopolymer material for drug delivery systems, food packaging materials to achieve medium barriers, and as a functional material for paper coating, specialty food product coating, and adhesives.

Acknowledgments

The authors gratefully acknowledge the Japan Society for the Promotion of Science for providing Obei-Tanki Fellowship, and the Natural Sciences and Engineering Research Council of Canada for providing NSERC Postdoctoral Fellowship to Dr. Neethirajan. The authors also thank the Food Nanotechnology Project of the Ministry of Agriculture, Forestry, and Fisheries of Japan for funding this study. Thanks are also due to Dr. Takeo Shiina, Distribution Engineering Laboratory, National Food Research Institute, Japan for providing access to the DLS equipment.

References

Aguilera JM, Stanley D. 1999. Microstructural Principles of Food Processing and Engineering. Maryland: Aspen Publishers, Inc.
Angellier-Coussy H, Putaux J, Molina-Boisseau S, Dufresne A, Bertoft E, Perez S. 2009. The molecular structure of waxy maize starch nanocrystals. Carbohyd Res 344:1558–66.
Atkin NJ, Abeysekera RM, Robards AW. 1998. The events leading to the formation of ghost remnants from the starch granule surface and the contribution of the granule surface to the gelatinization endotherm. Carbohyd Polym 36:193–204.
Baker A, Miles M, Helbert W. 2001. Internal structure of the starch granule revealed by AFM. Carbohyd Res 330:249–56.
Baldwin P, Adler J, Davies M, Melia C. 1998. High resolution imaging of starch granule surfaces by atomic force microscopy. J Cereal Sci 27:255–65.
Calvert P. 1997. Biopolymers – The structure of starch. Nature 389:338–9.
Cao X, Chen Y, Chang PR, Muir AD, Falk G. 2008. Starch-based nanocomposites reinforced with flax cellulose nanocrystals. eXPRESS Polym Lett 2:502–10.
Corre DL, Bras J, Dufresne A. 2010. Starch Nanoparticles: a review. Biomacromol 11:1139–53.
Couch JF, Naghski J, Krewson CF. 1946. Buckwheat as a source of rutin. Science 103:197–8.
Franciscus EG, Remigius OJJ, Herman F, Kornelis FG, Arjen B. 2004 Jan 13. Biopolymer Nanoparticles. U.S. patent 6,677,386.
Fredriksson H, Silverio J, Andersson R, Eliasson A, Aman P. 1998. The influence of amylose and amylopectin characteristics on gelatinization and retrogradation properties of different starches. Carbohyd Polym 35:119–34.
Gerard C, Colonna P, Buleon A, Planchot V. 2002. Order in maize mutant starches revealed by mild acid hydrolysis. Carbohyd Polym 48:131–41.
Hernandez-Munoz P, Lagaron J, Lopez-Rubio A, Gavara R. 2004. Gliadins polymerized with cysteine: effects on the physical and water barrier properties of derived films. Biomacromolecules 5:1503–10.
Huber K, BeMiller J. 1997. Visualization of channels and cavities of corn and sorghum starch granules. Cereal Chem 74:537–41.
Juszczak L, Fortuna T, Krok, F. 2003. Non-contact atomic force microscopy of starch granules surface. Part I. Potato and tapioca starches. Starch-Starke 55:1–7.
Kristo E, Biliaderis C. 2007. Physical properties of starch nanocrystal-reinforced pullulan films. Carbohyd Polym 68:146–58.
Le Corre D, Bras J, Dufresne A. 2010. Starch Nanoparticles: a Review.Biomacromolecules 11:1139–53.
Lindeboom N, Chang P, Tyler R. 2004. Analytical, biochemical and physicochemical aspects of starch granule size, with emphasis on small granule starches: a review. Starch-Starke 56:89–99.
Myers A, Morell M, James M, Ball S. 2000. Recent progress toward understanding biosynthesis of the amylopectin crystal. Plant Physiol 122:989–97.
Neethirajan S, Thomson D, Jayas D, White N. 2008. Characterization of the surface morphology of durum wheat starch granules using atomic force microscopy. Microsc Res Techniq 71:125–32.
Noda T, Takahata Y, Sato T, Suda I, Morishita T, Ishiguro K, Yamakawa O. 1998. Relationships between chain length distribution of amylopectin and gelatinization properties within the same botanical origin for sweet potato and buckwheat. Carbohyd Polym 37:153–8.
Parker ML, Kirby AR, Morris VJ. 2008. In situ imaging of pea starch in seeds. Food Biophys 3:66–76.
Raeker MO, Gaines CS, Finnery PL, Donelson T. 1998. Granule size distribution and chemical composition of starches from 12 soft wheat cultivars. Cereal Chem 75(5):721–8.
Raj B, Raj A, Kumar K, Siddarramaiah S. 2002. Moisture-sorption characteristics of starch/low-density polyethylene films. J Appl Polym Sci 84:1193–02.
Ridout MJ, Gunning, AP, Wilson, RH, Parker ML, Morris VJ. 2002. Using AFM to image the internal structure of starch granules. Carbohyd Polym 50:123–32.
Ridout MJ, Parker ML, Hedley CL, Bogracheva TY, Morris VJ. 2004. Atomic force microscopy of pea starch: origins of image contrast. Biomacromolecules 5:1519–27.
Rockland LB. 1960. Saturated salt solutions for static control of relative humidity between 5° and 40°C. Anal Chem 32:1375–6.
Shimoni E. 2008. Starch as an encapsulation material to control digestion rate in the delivery of active food components. Cambridge, UK: Woodhead Publishing Company.
Soral-Smietana M, Fornal L, Fornal J. 1984. Characteristics 351 of buckwheat grain starch and the effect of hydrothermal processing upon its chemical-composition, properties and structure. Starch-Starke 36:153–8.
Srichuwong S, Sunarti T, Mishima T, Isono N, Hisamatsu M. 2005. Starches from different botanical sources I: contribution of amylopectin fine structure to thermal properties and enzyme digestibility. Carbohyd Polym 60:529–38.
Stark J, Lynn A. 1992. Starch granules large and small. Biochem Soc Trans 20:7–12.
Szymonska J, Krok F, Tomasik P. 2000. Deep-freezing of potato starch. Int J Biol Macromol 27:307–14.
Szymonska J, Targosz-Korecka M, Krok F. 2009. Characterization of starch nanoparticles. J Phys Conf Ser 146:1–6.
Tang H, Ando H, Watanabe K, Takeda Y, Mitsunaga T. 2001. Physicochemical properties and structure of large, medium and small granule starches in fractions of normal barley endosperm. Carbohyd Res 330:241–8.